



ISSN: 2230-9926

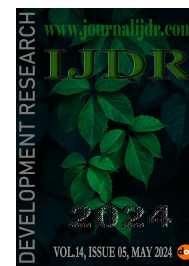
Available online at <http://www.journalijdr.com>

# IJDR

International Journal of Development Research

Vol. 14, Issue, 05, pp. 65741-65745, May, 2024

<https://doi.org/10.37118/ijdr.28338.05.2024>



RESEARCH ARTICLE

OPEN ACCESS

## FABRICATION OF COBALT FERRITE NANOPARTICLES WITH OKRA (*Abelmoschus esculentus*) EXTRACT IN A MICROWAVE REACTOR

Arthur Dantas Bergo de Lacerda<sup>1</sup>, Brunno Renato Farias Verçoza Costa<sup>2</sup>  
and Robson Roney Bernardo\*<sup>1</sup>

<sup>1</sup>Núcleo Multidisciplinar de Pesquisas em Nanotecnologia, NUMPEX-Nano, Campus UFRJ-Duque de Caxias Prof. Geraldo Cidade, Universidade Federal do Rio de Janeiro, Rodovia Washington Luiz, km 105. 25240-005, Duque de Caxias, RJ, Brazil; <sup>2</sup>Núcleo Multidisciplinar de Pesquisas, NUMPEX, Campus UFRJ-Duque de Caxias Prof. Geraldo Cidade, Universidade Federal do Rio de Janeiro, Rodovia Washington Luiz, km 105. 25240-005, Duque de Caxias, RJ, Brazil

### ARTICLE INFO

#### Article History:

Received 06<sup>th</sup> February, 2024

Received in revised form

17<sup>th</sup> March, 2024

Accepted 24<sup>th</sup> April, 2024

Published online 30<sup>th</sup> May, 2024

#### Key Words:

Cobalt ferrites; *Abelmoschus esculentus*;  
Microwave reactor; Microwave synthesis.

\*Corresponding author:  
Robson Roney Bernardo

### ABSTRACT

In recent years, metal oxide nanoparticles have been the object of study because of their unique optical, electronic, and magnetic properties. Cobalt ferrites ( $\text{CoFe}_2\text{O}_4$ ) are materials that have high magnetocrystalline anisotropy and coercivity and are used in several applications such as contrast agents for magnetic resonance imaging, biosensors, magnetic hyperthermia, and localized drug delivery. In the present work, the functionalization of the nanoparticles was performed with bioactives from okra extract (*Abelmoschus esculentus*). The objective of this work is the synthesis of cobalt ferrites using cobalt nitrate, iron nitrate, and okra juice in aqueous solution in an Anton Paar Monowave 200 microwave reactor using different parameters to determine the best reaction time and volume. Five syntheses were performed using different volumes and reaction times in the G30 tube of the reactor, and the following characterizations were made: dynamic light scattering (DLS), scanning transmission electron microscopy (STEM), zeta potential, and elemental analysis. The samples were identified as AD-1, AD-2, AD-3, AD-4, and AD-5, and the parameters used in each one were as follows: in AD-1, 12 mL of volume over 40 min of reaction; in AD-2, 8 mL over 20 min; in AD-3, 6 mL over 20 min; in AD-4, 15 mL over 90 min; and in AD-5, 15 mL over 40 min, all at a temperature of 110 °C. In DLS, the average sizes of the nanoparticles were as follows: AD-1 262 nm, AD-2 233 nm, AD-3 137 nm, AD-4 535 nm, and AD-5 627 nm. For average zeta potential, the following were obtained: AD-1 32 mV, AD-2 24 mV, AD-3 15 mV, AD-4 21 mV, and AD-5 15 mV. Therefore, it is evident that the use of okra bioactives favors the formation of nanoparticles, probably due to the presence of charged groups, and the synthesis in the microwave reactor was more successful when smaller volumes and shorter times were used, as in the AD-3 sample, due to the greater homogeneity and control of this synthesis method, thus making natural okra polymers potential substitutes for synthetic polymers for the synthesis of cobalt ferrites.

Copyright©2024, Arthur Dantas Bergo de Lacerda et al. This is an open access article distributed under the Creative Commons Attribution License, which permits unrestricted use, distribution, and reproduction in any medium, provided the original work is properly cited.

Citation: Arthur Dantas Bergo de Lacerda, Brunno Renato Farias Verçoza Costa and Robson Roney Bernardo, 2024. "Fabrication of Cobalt Ferrite Nanoparticles with Okra (*Abelmoschus esculentus*) Extract in a Microwave Reactor". International Journal of Development Research, 14, (05), 65741-65745

## INTRODUCTION

Nanoparticles (NPs) have been widely studied in recent decades because, due to their size on a nanometric scale, they have unique physical and chemical characteristics. The study, manipulation, and application of NPs provide great potential for new applications that can revolutionize all of humanity. Nanotechnology has slowly but profoundly taken control of different industries around the world, and the rapid development of nanoscience is proof that nanoscale production will soon be incorporated into almost all domains of science and technology (Malik, Muhammad & Waheed, 2023). However, one of the major barriers for the diffusion of nanotechnology is the difficulty of predicting the environmental risks

of the use of nanoparticles, especially those that use synthetic polymeric materials. For example, the possible toxicity of polymeric nanoparticles is a primary concern with their use in medicine (Abbad et al., 2021). Because of that, a lot of research is being conducted to align nanoscience with green chemistry, replacing the use of synthetic polymers with natural polymers, which are more attractive because they are cheap, biocompatible, chemically modifiable, biodegradable, and allow simple control of nanoparticle size and surface properties (Wilczewska et al., 2012). Metal oxide nanoparticles have been studied because of their unusual optical, electronic, and magnetic properties, which differ from those of other materials on a macrometric scale. Ferrites are materials obtained from iron oxide and have the formula  $\text{MeFe}_2\text{O}_4$ , where Me is a  $\text{NOX}^{+2}$  transition metal. Transition metals, such as cobalt and iron, have incomplete d-

orbitals in their electron configurations, which gives them unusual physicochemical characteristics when compared with other elements (Sridharan, 2016). In this sense, these metals can assume various oxidation states, which means that they can receive electrons and form bonds that form crystalline structures, as is the case with cobalt ferrite. It has a spinel-like crystal structure in which ions of different oxidation states are present in both tetrahedral and octahedral sites (Kingery, Bowen, Uhlmann, 1976). In addition, there are different ways to arrange the cations in those places: normal spinel or inverted spinel. In the case of  $\text{CoFe}_2\text{O}_4$  in a normal spinel conformation, as shown in Figure 1, the +2 cations occupy tetrahedral sites and +3 cations occupy octahedral sites, whereas in the inverted spinel conformation, as shown in Figure 2, all the cobalt cations assume octahedral positions along with half of the iron ions and the rest of the iron cations assume tetrahedral positions.

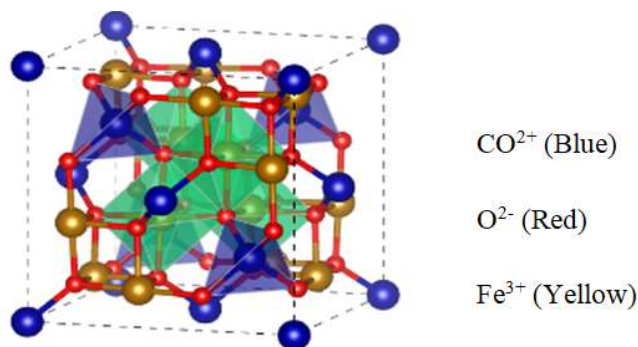


Fig. 1. Normal spinel (from the authors)

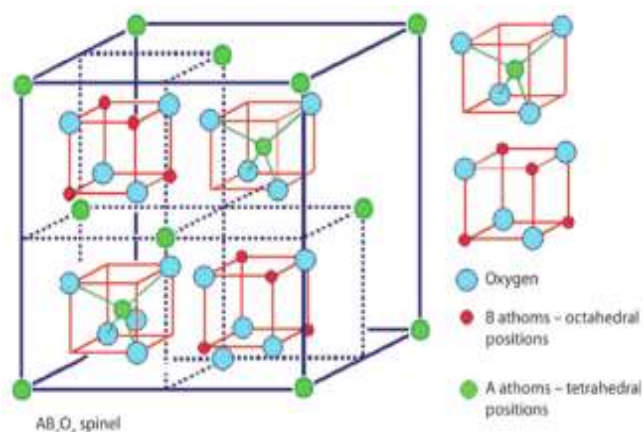


Fig. 2. Inverted spinel (Houshiar et al., 2014)

Cobalt ferrites are ferrimagnetic ceramic materials that can be hard or soft, have moderate magnetization and remanence due to the great interaction between metal ions (Maaz et al., 2007), have high magneto crystalline anisotropy and coercivity, and are used in a wide range of applications such as contrast agents for magnetic resonance imaging, biosensors, magnetic hyperthermia, and localized drug delivery (Júnior, 2015). The magnetic properties of this material depend on its size, shape, surface defects, binding surfaces, and temperature (Gubin, 2008). The functionalization of the nanoparticles was performed with bioactives from okra extract (*Abelmoschus esculentus*) to provide new properties for the nanoparticles and replace the use of synthetic polymers, following the principles of green chemistry. Okra was chosen because its extract is a mucilaginous substance similar to a viscous gel and contains several nutrients such as antioxidant agents, vitamins, proteins, mineral salts, and polysaccharides. The most commonly present polysaccharides are pectins, which are complex acidic heteropolysaccharides rich in galacturonic acid (Zhu et al., 2020). These pectins from okra are divided into three main types: homogalacturonan (HG), rhamnogalacturonan I (RG-I), and rhamnogalacturonan II (RG-II) (Willats, Knox, & Mikkelsen, 2006).

## MATERIAL AND METHODS

**Preparation of the Reagents:** Cobalt nitrate, iron nitrate, and okra extract were used as reagents in the synthesis of cobalt ferrites.

**Preparation of the *Abelmoschus esculentus* extract:** Okra was purchased from a local market. For each synthesis, three okra pods were cut in half lengthwise and their mesocarps and seeds were extracted with a scraper, macerated with mortar and pestle, and placed into a beaker with 12.5 mL of Milli-Q water. The solution was left to rest for 30 min until the water had a mucilaginous and optically translucent texture. After that time, the okra extract was sifted into another beaker, thus being ready for reaction.  $\text{Co}(\text{NO}_3)_2$  (0.218325 g) in 6.25 mL of Milli-Q water in one beaker ( $M = 0.48$  mol/L) and 0.606 g of  $\text{Fe}(\text{NO}_3)_3$  in 6.25 mL of Milli-Q water in another beaker ( $M = 0.96$  mol/L) were used.

**Synthesis in the Microwave Reactor:** Five syntheses were made in the G30 tube of the Anton Paar Monowave 200 reactor: AD-1, AD-2, AD-3, AD-4, and AD-5. The parameters used in the reaction are shown in Box 1 below:

Parameters	AD-1	AD-2	AD-3	AD-4	AD-5
$\text{Co}(\text{NO}_3)_2$ (mL)	4	4	2	5	5
$\text{Fe}(\text{NO}_3)_3$ (mL)	4	2	2	5	5
Okra Extract (mL)	4	2	2	5	5
Total Volume (mL)	12	8	6	15	15
Temperature ( $^{\circ}\text{C}$ )	110	110	110	110	110
Time (min)	40	20	20	90	50

### Box 1. Sample reaction conditions

**Sample Purification:** After synthesis, the samples were centrifuged at 1200 RPM for 10 min. The supernatant was discarded, and a second round of ethanol centrifugation was performed using the same parameters as the first. Next, the samples were dried at  $80^{\circ}\text{C}$  for 24 h and taken to a muffle at  $500^{\circ}\text{C}$  for 2 h.

**Dynamic Light Scattering (DLS):** In this study, an Anton Paar Litesizer DLS 500 device, disposable cuvettes, and aqueous solution with transmittance between 60% and 80% were used.

**Zeta Potential:** Zeta potential was also measured on a Litesizer DLS 500 device with Omega cuvettes.

**Scanning Transmission Electron Microscopy (STEM):** STEM was used to analyze the cobalt ferrite nanoparticles. For analysis, the samples were inserted and submitted to the Tescan VEGA3 device equipped with a STEM detector at the Numpex-Bio laboratory of UFRJ Duque de Caxias.

**Elemental Analysis:** Elemental analysis was also performed on a Tescan VEGA3 device, which also performs energy-dispersive X-ray spectroscopy (EDS). Elemental mapping and chemical analysis were performed.

## RESULTS AND DISCUSSION

Because of their wide range of applications, cobalt ferrites are considered extremely important materials and highly promising for the technical and scientific advances of humanity. Okra is widely cultivated in the tropics, subtropics, and temperate regions around the world, including Africa, Asia, and North America. Like many other biopolymers, its physicochemical properties, low production cost, good regulatory acceptance, and availability make it an excellent choice for various applications in the pharmaceutical and food industries (Ghori et al., 2014; Vincken et al., 2003). In this study, cobalt ferrite particles were produced with okra extract and had very distinct characteristics due to changes in reaction parameters.

**Microwave Reactor:** A microwave reactor consists of the emission of electromagnetic waves in the microwave spectrum, which have frequencies from 0.3 to 300 GHz. Conventional household microwave reactors, for example, have a frequency of 2.45 GHz. Microwave frequencies are low, so they cannot break interatomic bonds (Neas, Collins 1988). Therefore, the energy for the reaction to occur comes from the dielectric heating that takes place when the electric dipole of a polar molecule varies according to the oscillating electric field of the microwave reactor, generating friction between the molecules and heat. In addition, in the case of ions, ionic conduction occurs with variations in the electric field, generating collisions and, consequently, heat. As a result, there is a sudden homogeneous increase in temperature, causing the atoms to rotate and diffuse rapidly, hence increasing the number of collisions between them. Thus, it is possible for reactions that take hours in conventional reactors to be carried out in minutes in a microwave reactor with the reaction rate following the Arrhenius equation. In the case of chemical reactors, the reaction is performed at controlled pressure and with magnetic agitation to make the temperature even more homogeneous (Kremsner & Stadler, 2018). Therefore, with all those factors, sufficient energy is generated for the formation of cobalt ferrite and its byproducts to occur.

**DLS and Zeta Potential:** DLS, or dynamic light scattering, is a technique used to detect average particle sizes from 0.3 nm to 10  $\mu\text{m}$  from a polarized laser that hits the cuvette containing the sample in aqueous solution. The beams are then detected and analyzed based on the polarization scattering angle and scattering volume in a given region. Zeta potential, on the other hand, is a measure of the surface charge of the particles. When its modulus is above 30, it means that the particles are stable and do not tend to aggregate, whereas if the modulus is less than that value, the particles tend to aggregate. The results of those analyses are shown in Box 2 and Table 1 below: In a study published by Kombaiah *et al.* (2017), cobalt ferrite syntheses were conducted using okra extract by conventional heating method and by microwave heating in a 2.54 GHz 850 W domestic microwave. In the conventional heating method, the nanoparticles had sizes of 300–500 nm, whereas the sizes in microwave heating were 5–50 nm. However, the nanoparticles synthesized in the microwave oven were not calcined (Kombaiah *et al.*, 2017). In this context, the nanoparticles synthesized in this work have similar size ranges when compared with those of that previous study. From the DLS and STEM analyses, we can conclude that the best samples were AD-1, AD-2, and AD-3; however, AD-2 was the only one that was not magnetic. The appearance of that sample was lighter than that of the other samples, which were very dark.

Results	AD-1	AD-2	AD-3	AD-4	AD-5
Hydrodynamic diameter(nm)	262	233	137	535	627
Polydispersity Index(%)	24.1	28.1	28.8	28.4	32.2
Transmittance(%)	76.9	68.8	77.5	68.4	61.6
Mean Zeta Potential(mV)	-32	-24	-15	-21	-15

Box 2. Average DLS and zeta potential results

Sample	Peak 1(nm)	Area 1 (%)	Peak 2(nm)	Area 2(%)	Peak 3(nm)	Area 3(%)
AD-1	244.9	73.67	2.92	23.35	2611	2.98
AD-2	400	73.09	81.73	26.91	//	//
AD-3	232.9	73.13	2325	6.41	31.40	20.47
AD-4	553.8	75.74	1.03	24.26	//	//
AD-5	590.1	58.66	183.8	27.13	13055	14.22

Table 1. Size signs in the DLS

## STEM

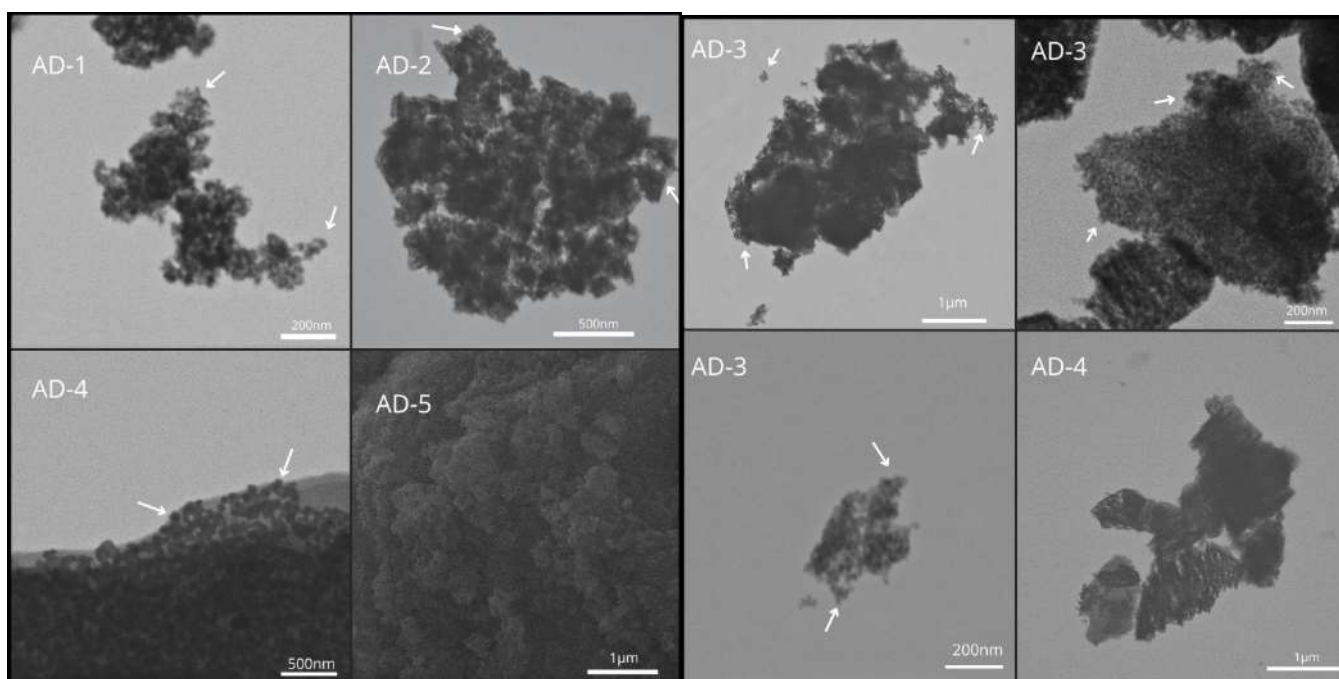
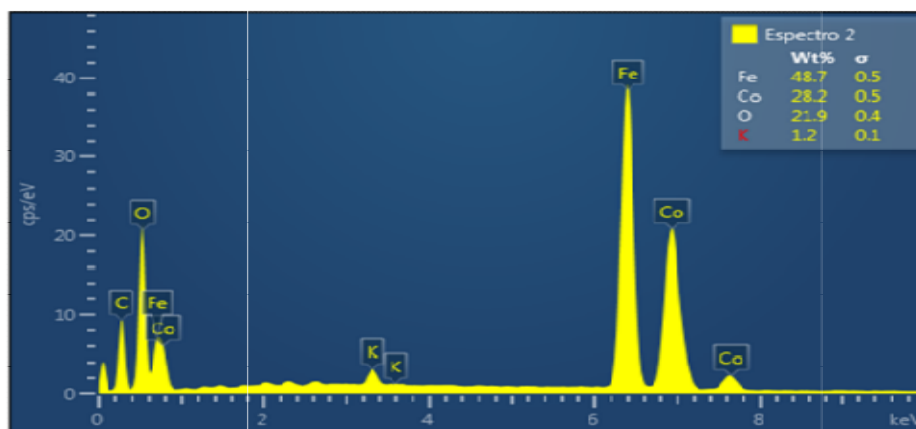


Fig. 3. Scanning transmission electron microscopy of five samples: AD-1, AD-2, AD-3, AD-4, and AD-5



Graph 1. Elemental analysis of AD-1

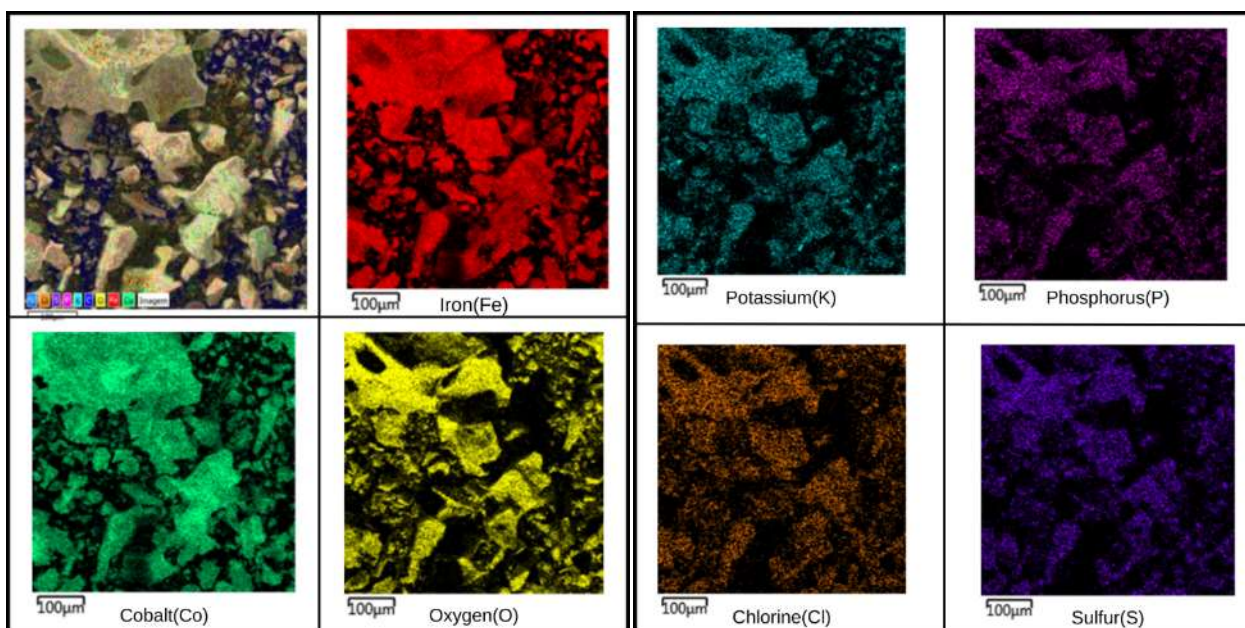


Fig. 7. Mapping in AD-1 EDS.EE

It is possible to observe a trend of aggregation of these nanoparticles, although they have signs of small nanoparticles in the DLS. Microwave synthesis of cobalt ferrites using okra bioactives yielded smaller grains, larger surface areas, aggregation, and uniform distribution, and AD-1, AD-2, and AD-3 were similar to the cobalt ferrite nanoparticles synthesized by Kombaiah *et al.* (2017). A similar aggregation pattern is seen using other synthesis methods when compared to the present work, such as the synthesis of cobalt ferrites by coprecipitation and precipitation in the publication by Houshiar *et al.* (2014). Comparing the AD-1 images, Figure 5b by Kombaiah *et al.* (2017), and Figure 3b by Houshiar *et al.* (2014), we observed nanoparticles with spherical sizes ranging from 10 to 200 nm. Differences in synthesis, such as the solvents used, time in the reactor, use of surfactants and bioactives, and calcination, are factors that directly interfere with the final size of nanoparticles. The higher the treatment temperature of the sample, the more ion diffusion is facilitated, leading to the formation of nanoparticles of more continuous forms throughout the material (Purnama., Wijayanta, Suharyana, 2019) to reduce the total boundary energy, surface area, and number of pores (Callister, 2008). Figure 1 by Rodrigues *et al.* (2023) is an example of cobalt ferrite made using kiwi bioactives, where there is apparently a size variation of 200 nm at 5  $\mu\text{m}$  (Rodrigues *et al.*, 2023) and cuboid shape, differing from the magnetic nanoparticles made with okra, which apparently became smaller and spherical.

**Elemental Analysis:** From the DLS analysis and STEM results, the AD-1 sample was analyzed by energy dispersive X-ray spectroscopy

(EDS) to determine the chemical composition of the sample. Elemental mapping was carried out, which uses characteristic x-rays generated by an electron beam to visualize the distribution of the constituent elements in the sample, giving the composition of the material in layers under a photo, as shown in Figure 6. The analyzer, on the other hand, uses x-rays to detect the mass average of the amount of elements present, as shown in Graph 1. Figure 7 shows the results of EDS mapping of AD-1. The first image from the left box is the photo with the overlapping element layers, and the following photos are the separate element layers: iron (Fe), cobalt (Co), oxygen (O), potassium (K), phosphorus (P), chlorine (Cl) and sulfur (S). We can see a large amount of iron, cobalt, and oxygen overlapping the particles in the sample, which indicates a high possibility of it being cobalt ferrite. In addition, the presence of the other elements probably comes from okra extract, considering that potassium and phosphorus are elements present in that vegetable (Ani *et al.*, 2012).

## CONCLUSION

In this study, it was shown that the use of bioactives from okra extract favors the formation of nanoparticles in the cobalt ferrite synthesis reaction in a microwave reactor. In addition, from the results, it can be concluded that the parameters used in AD-1 and AD-3 are ideal for the synthesis of this material using that plant as functionalization in this synthesis method, and the results of the characterizations were compatible with the results of previous published studies of the same material.

## Acknowledgments

This work was supported by Fundação de Amparo à Pesquisa do Estado do Rio de Janeiro (FAPERJ) no Programa Redes de Pesquisa em Nanotecnologia no Estado do Rio de Janeiro (E-26/010.000981/2019) and Conselho Nacional de Desenvolvimento Científico e Tecnológico (CNPq/UFRJ- PIBIC).

## REFERENCES

- Abbad, S., Wang, C., Waddad, A., Lv, H., Zhou, J. 2015. Preparation, in vitro and in vivo evaluation of Polymeric nanoparticles based on hyaluronic acid-Poly(butyl cyanoacrylate) and D-alpha-tocopheryl Polyethylene glycol 1000 succinate for tumor-targeted delivery of Morin hydrate. *International Journal of Nanomedicine*, 10, 305-320. [10.2147/IJN.S73971](https://doi.org/10.2147/IJN.S73971).
- Ani, J.U., Nnaji, N.J., Okoye, C. O. B., Okukwuli, O.D. 2012. The Coagulation Performance of Okra Mucilage in An Industrial Effluent by Turbidimetry. *Int. J. Chem. Sci.*, 10(3), 1293-1308.
- Callister, W. D. J. *Ciência e Engenharia dos Materiais, uma Introdução*. 7. ed. [S.l.]: Ed. Guanabara, 2008. 589 p. 57 e 58.
- Ghori, M. U.; Alba, K; Smith, A. M.; Conway, B. R; Kontogiorgos, V. 2015. Okra extracts in pharmaceutical and food applications. *Food Hydrocolloids*, 42(3), 342-7. <http://dx.doi.org/10.1016/j.foodhyd.2014.04.024>
- Gubin, S.P. *Magnetic Nanoparticles*. editora Wiley-VCH Verlag, Weinheim, Germany, 2009.
- Houshiar, M., Zebhi, F., Razi, Z. J., Alidoust, A. Askari, Z. 2014. Synthesis of cobalt ferrite (CoFe<sub>2</sub>O<sub>4</sub>) nanoparticles using combustion, coprecipitation, and precipitation methods: A comparison study of size, structural, and magnetic properties. *Journal of Magnetism and Magnetic Materials*, 371, 43-8. <http://dx.doi.org/10.1016/j.jmmm.2014.06.059>.
- Junior, J.V. 2015. Síntese por Sol-Gel de Ferrita de Cobalto e sua Caracterização Microestrutural e de Propriedades Magnéticas. Tese de mestrado. Programa de Pós-Graduação de Engenharia de Minas, Metalúrgica e de Materiais – PPGE3M, Escola de engenharia, UFRS.
- Kingery, W. D., Bowen, H. K., Uhlmann, D. R. Introduction to Ceramics. *John Wiley & Sons*, New York, EUA, 1976.
- Kombaiah, K., Vijaya, J. J., Kennedy, L. J., Bououdina, M., Ramalingam, R.J., Al-Lohedan, H.A. 2018. Okra extract-assisted green synthesis of CoFe<sub>2</sub>O<sub>4</sub> nanoparticles and their optical, magnetic, and antimicrobial properties. *Materials Chemistry and Physics*, 15, 410-9. [DOI.10.1016/j.matchemphys.2017.10.077](https://doi.org/10.1016/j.matchemphys.2017.10.077)
- Kremsner, J. M., Stadler, A. A. *Chemist's Guide to Microwave Synthesis*, 3th edition, 2018
- Maaz, K., Mumtaz, A., Hasanain, S.K, Ceylan, A. 2007. Synthesis and magnetic properties of cobalt ferrite (CoFe<sub>2</sub>O<sub>4</sub>) nanoparticles prepared by wet chemical route. *Journal of Magnetism and Magnetic Materials*, 308(2), 289-295.
- Malik, S., Muhammad, K., Waheed, Y. 2023. Nanotechnology: A Revolution in Modern Industry. *Molecules*, 28(2), 661. [doi: 10.3390/molecules28020661](https://doi.org/10.3390/molecules28020661).
- Neas, E. & Collins, M. *Microwave Heating - Theoretical Concept and Equipment Design*, American Chemical Society, 1988
- Purnama, B., Wijayanta, A.T., Suharyana. 2019. Effect of calcination temperature on structural and magnetic properties in cobalt ferrite nano particles. *Journal of King Saud University – Science*, 31(4), 956-960. [doi.org/10.1016/j.jksus.2018.07.019](https://doi.org/10.1016/j.jksus.2018.07.019).
- Rodrigues, G. C., de Lima, A. C. C., Attela, G. C., Bernardo, R. R. 2023 Green synthesis of magnetic nanoparticles of cobalt ferrite with kiwi (*Actinidia deliciosa*) and its activity against the proliferation of *Trypanosoma cruzi*. *Journal of Engineering Research*, 3(7). [DOI10.22533/at.ed.317372315032](https://doi.org/10.22533/at.ed.317372315032).
- Sridharan, K. 2016. The electromagnetic spectrum. *Spectral Methods in Transition Metal Complexes*; Chapter 1, 1–12. <http://dx.doi.org/10.1016/B978-0-12-809591-1.00001-3>.
- Vincken, J. P., Schols, H. A., Oomen, R.; Beldman, G., Visser, R., Voragen, A. G. J. 2003. Pectin: the hairy thing: evidence that homogalacturonan is a side chain of rhamnogalacturonan I. *Advances in pectin and pectinase research*, 91-105.
- Wilczewska, A., Niemirowicz, K., Markiewicz, K., Car, H. 2012. Nanoparticles as drug delivery systems. *Pharmacol. Rep.* 64(5), 1020-37. [doi: 10.1016/s1734-1140\(12\)70901-5](https://doi.org/10.1016/s1734-1140(12)70901-5).
- Willats, W. G. T., Knox, J. P., Mikkelsen, J. D. 2006. Pectin: new insights into an old polymer are starting to gel. *Trends in Food Science & Technology*, 17(3), 97-104.
- Zhu, X.M., Xu, R., Wang, H., Chen, J.Y., Tu, Z.C. 2020. Structural Properties, Bioactivities, and Applications of Polysaccharides from Okra [*Abelmoschus esculentus* (L.) Moench]: A Review. *J. Agric. Food Chem.* 68, 48, 14091–14103

\*\*\*\*\*